International Journal of Biological Macromolecules 164 (2020) 3943–3952

Contents lists available at ScienceDirect

International Journal of Biological Macromolecules

journal homepage: http://www.elsevier.com/locate/ijbiomac

Nano-interface driven electrochemical sensor for pesticides detection based on the acetylcholinesterase enzyme inhibition

Amar Pal Singh [a,b], Sapna Balayan [c], Vinita Hooda [d], R.K. Sarin [e], Nidhi Chauhan [c,*]

[a] Amity Institute of Forensic Sciences (AIFS), Amity University Uttar Pradesh (AUUP), Noida 201313, India
[b] Forensic Science Laboratory, Govt. of NCT of Delhi, Veera Centre, Sector-23, Rohini, Delhi-110099, India
[c] Amity Institute of Nanotechnology (AINT), Amity University Uttar Pradesh (AUUP), Noida 201313, India
[d] Department of Botany, M. D. University, Rohtak 124001, Haryana, India
[e] Andhra Pradesh Forensic Science Laboratory (APFSL), Police Tech Tower, Mangalgiri, Guntur (Dt.), Andhra Pradesh 522503, India

ARTICLE INFO

Article history:
Received 21 June 2020
Received in revised form 27 August 2020
Accepted 28 August 2020
Available online 01 September 2020

Keywords:
Zinc oxide nanoflowers
Reduced graphene oxide
Acetylcholinesterase
Biosensor
Pesticides

ABSTRACT

Forensic Science Laboratories usually receive numerous cases of suicidal, accidental, and homicidal poisoning most often involving organophosphorus (OP) pesticides. The toxicity of the OP pesticides arises due to their ability to inhibit the activity of acetylcholinesterase (AChE), a cholinergic enzyme that is essential for the proper functioning of the central nervous system. Conventional techniques which are currently in use for pesticide detection are time-consuming, need upskilled technicians as well as suffer from low sensitivity. Therefore, the more rapid and sensitive electrochemical biosensors based on the principle of AChE enzyme inhibition have emerged out to be a simple and promising alternative to the conventional techniques. Since, most of the time, the poison isolated from biological material in poisoning cases is in nM quantities, an attempt has been made for the development of biosensor with enhanced sensitivity in the nM range using reduced graphene oxide (rGO) and zinc oxide nanoflowers (ZnONFs). The rGO and ZnONFs were synthesized chemically and deposited electrochemically on the Au electrode. AChE was immobilized onto this prepared nano-interface (ZnONFs/rGO/Au) through chitosan and glutaraldehyde cross-linking. The fabricated sensor was characterized step by step with cyclic voltammogram and electrochemical impedance spectroscopy. This advanced nanomaterials based techniques has been explored for detecting pesticides in visceral samples. The limit of detection (LOD) for the present sensor was 0.01 nM for OP pesticides.

1. Introduction

The injudicious application of organophosphorus (OP) pesticides in the agricultural fields has not only polluted the environment but is also responsible for high pesticide poisoning cases across the globe causing serious health problems [1–4]. The deadly toxic OP compounds affect the nervous system by hampering the functioning of acetylcholinesterase (AChE) by blocking the active serine site covalently and by disturbing the normal acetylcholine (ACh) mediated neurotransmission [5,6]. Consequently, strong cholinergic symptoms are observed in human beings with the manifestation of muscarinic (salivation, urination, miosis, diarrhea, and excess lacrimation), nicotinic (cramping, muscle fasciculation, weakness) and Central Nervous System effects (respiratory paralysis, restlessness, and death) [7]. In India, deaths by OP poisoning and associated illnesses are observed at a large scale [8]. The World Health Organization has also reported that in developing countries approximately 3 million cases and 220,000 deaths per year could be attributed due to pesticide poisoning. Alongwith this, a rise in the number of OP pesticides associated with homicidal and accidental or suicidal death cases is also alarming. Globally, about 260,000 deaths per year occur due to self-poisoning and in these cases, detection, quantification, and identification of the toxic chemical in postmortem samples are needed to ascertain the cause of death and decide the course of the criminal investigation [8–10]. In other non-lethal poisoning cases, recognition of the responsible toxin is crucial for deciding the course of medical treatment and saving the life of the patient.

Traditionally, the detection of OP compounds is carried out by various laboratory-based chromatographic techniques which are not only complex, costly, and time-consuming but also require trained personnel, complex sample preparation, and high-cost equipment [11,12]. Moreover, the poison isolated from biological material in poisoning cases generally is in the nM quantities, which may not be detected by the conventional methods due to their low sensitivity. A simple, sensitive, and selective platform coupled with the possibility of onsite detection is ideal to be used for such purposes. The biosensors based on the transduction principle offer one such platform [13–19]. In recent years, the OP pesticide biosensors developed with AChE inhibition

* Corresponding author.
E-mail address: nchauhan1@amity.edu (N. Chauhan).

https://doi.org/10.1016/j.ijbiomac.2020.08.215
0141-8130/

principle have gained popularity due to their ultra-sensitive nature and simplicity [20]. Further, the use of biocompatible nanomaterials in the biosensors improves their performance by augmenting the surface area needed for AChE immobilization, enhancing the electrical conductivity and sensitivity, and reducing the response time [21–26]. Considering this, several biosensors have so far been constructed for OP pesticide detection that utilized a diverse range of simple or composite nanomaterials. The electrochemical biosensor based on platinum-palladium N-doped carbon shell (PtPd@NCS) nanocomposite yielded quite a lower detection limit, the values being 7.9×10^{-15} M for malathion, 7.1×10^{-14} M for chlorpyrifos and for parathion methyl as 8.6×10^{-15} M [27]. Further, an ultrasensitive biosensor was constructed on the metal-organic framework with Pt—Zr nanocomposites (Pt@UiO66-NH_2) with a limit of detection (LOD) as 4.9×10^{-15} M for malathion [28]. An ultrathin disposable biosensor for paraoxon sensing was designed [29]. The sensor utilized the multi-dimensional nanocomposites (MXene/Au-Pd) as the functional platform for AChE immobilization and pesticide sensing and exhibited a low LOD of 1.75 ng/L.

Amongst the nanomaterials reduced graphene oxide (rGO) as a planar one atom thick sheet also presents impressive electrical conductivity due to a large number of electroactive sites, enhanced surface area, good mechanical and thermal strength, and a natural biocompatible environment. It is a promising material for immobilizing enzymes in chemical and biological sensor applications [30]. Furthermore, zinc oxide nanoflowers (ZnONFs) are also considered to be a suitable matrix for biosensing platforms because of their large interfacial areas supporting enhanced enzyme loading, biomimetic, catalytic, and fast electron transfer properties [31]. The synergistic effect of both the nanomaterials, if used together, is expected to enhance the sensitivity and linear range of the OP pesticide detection. In addition to the rGO and ZnONFs, the electrode was also modified with chitosan (CHIT) that offers excellent biocompatibility, good adhesion, and exceptional film-forming capabilities needed for efficient enzyme immobilization [32].

Hence, in the present work, the Au electrode suitably modified with the rGO, ZnONFs, and CHIT has been employed for AChE immobilization and electrochemical sensing of OP pesticides of forensic interest in the visceral samples. The accomplishment of the developed biosensor was assessed in terms of its linearity, LOD, reproducibility, and stability.

2. Experimental measurements

2.1. Chemicals and equipment

Acetylcholinesterase (AChE) enzyme, acetylthiocholine chloride (ATCl), 2-pyridine aldoxime methiodide (2-PAM), CHIT and glutaraldehyde were procured from Sigma Chemical Co., USA. Monocrotophos and Au electrode wire of dimension (15 mm × 0.5 mm) (23 carats) were obtained from the domestic vendor. The ZnONFs and rGO nanomaterials were synthesized in the laboratory by chemical methods. Distilled water (DW) was used throughout while performing the experiments.

Electrochemical characterization of the biosensor was done by Cyclic voltammetry (CV), Square wave voltammetry (SWV), and Electrochemical impedance spectroscopy (EIS). The electrochemical cell setup consisted of a three-electrode system, including an auxiliary (Platinum), reference (Ag/AgCl), and a working electrode on a potentiostat (SP-150, Biologics with EC-Lab software). For studying the surface morphology of the modified electrodes, Scanning Electron Microscopy (SEM) and Energy-dispersive X-ray spectroscopy (EDX) (ZEISS EVOHD) were performed at AIARS, Amity University, Noida, UP, India.

2.2. Synthesis of rGO

The rGO was synthesized chemically, using a modified Hummer's method with graphite powder (as a precursor) [33]. A 30 mL solution of sulphuric acid (98%, mass percent) was added to the graphite powder (2 g) under continuous stirring for 1 h. Thereafter, the solution was kept at 35 °C for 1 h in a water bath and stirred continuously while adding potassium permanganate ($KMnO_4$) (6 g). After that, DW water (100 mL) was added and continuous stirring for 2 h was carried out. Then, 110 mL solution of hydrogen peroxide (30%) was added to the above solution. The 5% hydrochloric acid (HCl) was used for washing the dark brown solution obtain to remove metal ions and washing was done until the solution pH was neutral. rGO precipitate was collected and kept for drying at 60 °C for 24 h.

2.3. Synthesis of ZnO nanoflowers (ZnONFs)

ZnONFs were synthesized using the precipitation method [34]. Sodium hydroxide (NaOH) and anhydrous zinc sulfate ($ZnSO_4 \cdot 7H_2O$) in a ratio of 1:2 M were added in 100 mL DW, the NaOH solution was gradually added into $ZnSO_4$ solution under continuous stirring. A pH of 12 was maintained for the solution and it was stirred overnight. The precipitate thus obtained was washed thrice with DW and once with ethanol. The precipitate was dried at 100 °C and calcinated at 500 °C for 3 h to get the ZnONFs.

2.4. Nano-electrodeposition of conducting material over Au electrode

The bare electrode (Au) was washed with the Piranha solution (H_2SO_4 and H_2O_2 in a ratio of 3:1) followed by washings with DW. Electrodeposition of rGO on the Au electrode was done with CV in a potential range from (0 to −1 V), for 10 cycles with scan rate 50 mV/s [35]. The electrodeposition of the ZnONFs was performed in a solution of the ferro/ferri mediator. A solution of 1 g of ZnONFs in 5 mL of ethanol and 5 mL of ferro/ferri mediator solution was prepared and sonicated for 1 h. The electrodeposition of ZnONFs on the modified rGO/Au electrode was carried out in a potential range (−1 to −1.2 V) for 10 cycles at a constant scan rate of 50 mV/s. For enzyme immobilization, the ZnONFs/rGO/Au electrode was modified with CHIT solution (0.075 g CHIT in 5 mL of acetic acid) and 2.5% glutaraldehyde (1 mL of 25% glutaraldehyde in 9 mL of DW). This activated ZnONFs/rGO/Au electrode was immersed in 1 mL of AChE enzyme solution (5 mg protein/mL) for 12 h. Then the modified AChE@CHIT/ZnONFs/rGO/Au electrode was washed with DW thrice and used as such for further experiments (Scheme 1).

2.5. Electrochemical measurement for the modified AChE@CHIT/ZnONFs/rGO/Au electrode towards the substrate

For the electrochemical study, a three-electrode system was adopted by taking auxiliary (platinum), reference (Ag/AgCl), and working (AChE@CHIT/ZnONFs/rGO/Au) electrode connected with a potentiostat. The apparatus was stabilized at +0.2 V for 15 s till a steady current was observed. A 100 μL solution of ATCl (0.1 nM) was added in ferro/ferri mediator solution and the current was measured by supplying +0.2 V. Due to the current flow, ATCl was enzymatically hydrolyzed to thiocholine which further dimerized into a disulphide compound. The AChE enzyme activity was measured with the CV technique at different concentrations of ATCl substrate (1.0 nM, 10 nM, 50 nM, 100 nM, 500 nM, 750 nM, and 1000 nM).

2.6. Nanoelectrochemistry for pesticide detection

The AChE@CHIT/ZnONFs/rGO/Au biosensor oxidized the ATCl substrate into thiocholine and the signal was enhanced. In the presence of OP pesticides, the enzyme AChE on the biosensor was blocked and conversion of ATCl substrate stopped due to the inhibition of the enzyme. The inhibition of AChE by OP pesticide was calculated for different concentrations of the pesticide using the modified AChE@CHIT/ZnONFs/rGO/Au electrode. The electrode was immersed in the pesticide (Monocrotophos) solution for 10 min, and then the electrode was

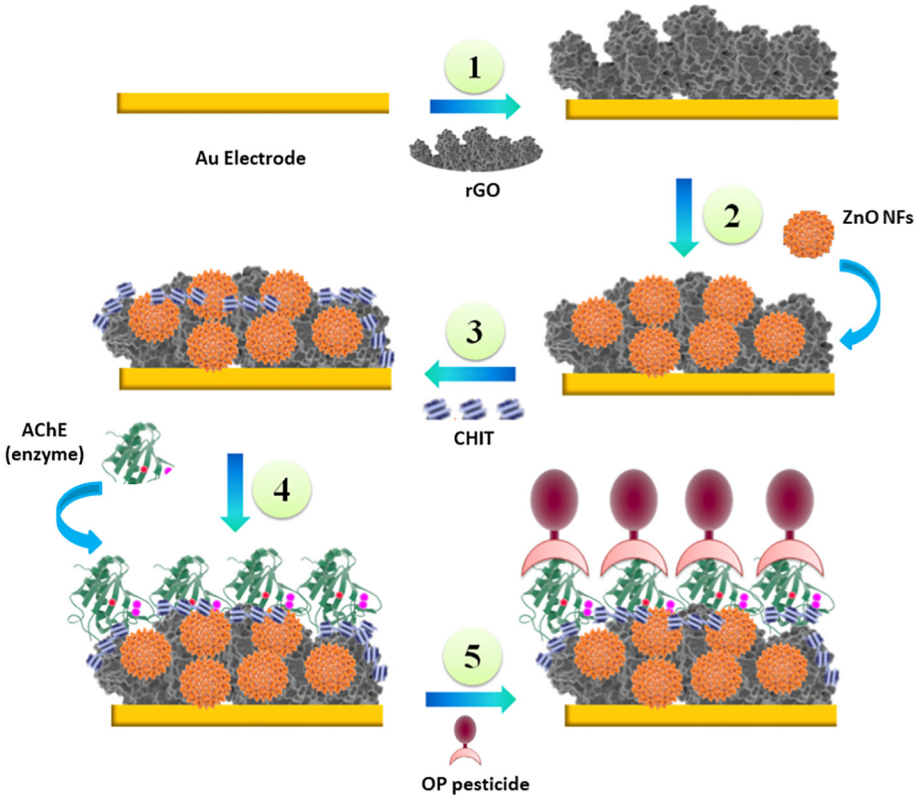

Scheme 1. Schematic illustration of the preparation of enzyme and nanocomposite modified Au electrode (working electrode). Step-1: Electrochemical deposition of rGO onto the Au electrode. Step-2: Electrochemical deposition of ZnONFs onto the rGO/Au electrode. Step-3: Spread the chitosan (CHIT) solution over the ZnONFs/rGO/Au electrode. Step-4: Immobilization of AChE (enzyme) onto the CHIT/ZnONFs/rGO/Au electrode through glutaraldehyde cross-linking. Step-5: Pesticide inhibited the activity of AChE@CHIT/ZnONFs/rGO/Au electrode.

dipped in the solution of the mediator containing 20 mL of ferro/ferri (10 mL each) and 1 mL of ATCl (1.0 nM) and electrochemical measurements for the sensor were performed. Analysis was carried out for standard pesticides solutions i.e. Monocrotophos with different concentrations: 0.01 nM, 0.1 nM, 10 nM, 50 nM, 75 nM and 100 nM.

2.7. Preparation of viscera sample for analysis

For analysis, 20 pesticide poisoning samples were collected from Forensic Science Laboratory, Govt. of NCT of Delhi, India. For sample preparation, about 1 g viscera was crushed using a homogenizer in 1.5 mL of 1 M Tris buffer at pH 4.7. After 60 min of incubation at 4 °C and centrifugation at 3000 rpmg for 10 min, 1 mL of the supernatant was used for the electrochemical measurements as mentioned before by just replacing the ATCl substrate with this prepared supernatant.

2.8. Enzyme reactivation

OP pesticide blocked the enzyme - AChE present at the working electrode due to the formation of a bond between AChE and OP pesticide. For further experimentation, reactivation of the biosensor was imperative. The electrode was reactivated by breaking the AChE-OP pesticide bond by dipping AChE@CHIT/ZnONFs/rGO/Au electrode into the solution consisting of 2-PAM (4.0 mM) dissolved in 2 mL of DW for 5 min. The electrode thus obtained was electrochemically examined with 1.0 nM analyte (ATCl).

3. Results and discussions

3.1. Characterization of the Nanointerface

The rGO suspension was characterized by High-resolution transmission electron microscopy (HR-TEM) as illustrated in Supplementary Fig. 1. The surface clearly shows the lattice fringes of rGO sheets with different thickness at 200 nm. The dark shade area in the image shows the thick stacking of the graphene layer.

The successful modification of the Au electrode with rGO, ZnONFs, and the enzyme in a successive manner was confirmed by SEM and EDX spectroscopy. The surface morphology of ZnONFs was also studied by SEM which has been depicted in Fig. 1A. The image depicts the uniform flower-like structure of ZnONFs, while the enlarged image shows an individual flower composed of the nanorods with a sharp tip. The insert confirms the size of single ZnONF to be around 100 nm. The stepwise modification of the working electrode from bare surface of the Au electrode, presence of a wrinkled sheet of rGO onto the Au surface, deposition of ZnONFs over the rGO/Au surface and finally the deposition of globular structures of the immobilized enzyme on the ZnONFs/rGO/Au electrode can be clearly seen in Fig. 1B (i) to (iv) respectively. All four images in Fig. 1B are distinguishable from each other and hence present clear evidence of the efficient stepwise modification of the working electrode.

Energy-dispersive X-ray spectroscopy (EDX) of the moderated electrode was done step by step to check the deposition of the nanomaterials on the working electrode. The EDX spectra confirm the presence of Au in Fig. 1C (i) with 100% weight percentage (wt%), Fig. 1C (ii) shows the peaks for carbon (C) and potassium (K) the expected elements for rGO with 100% and the peaks obtained in Fig. 1C (iii), confirms the presence of Zn and Au with elemental constitutes of

rGO (C and K) the measured weight ratio of C—K, Zn and Au were recorded as 21.96, 15.54, and 62.5 wt% respectively, showing the Au electrode was decorated with ZnONFs/rGo nanocomposite.

3.2. Electrochemical behavior of AChE@CHIT/ZnONFs/rGO/Au electrode

The moderated Au electrode was subjected to electrochemical measurements using a cyclic voltammogram in the −0.2 to 0.6 V potential range with a constant scan rate of 20 mV/s. Fig. 2 shows the cyclic voltammogram for the bare Au electrode (i), ZnONFs deposited on Au electrode (ii), rGO deposited Au electrode (iii), ZnONFs decorated rGO/Au electrode (ZnONFs/rGO/Au electrode) (iv), and the enzyme loaded ZnONFs/rGO/Au electrode (v). For performing the reaction Na_3PO_4 buffer solution (0.5 mM, pH 7.0) was mixed with 5 mM ferro/ferri mediator solution. The oxidation peak for the bare electrode was observed at 0.09 mA whereas for the nanomaterial modified electrode it increased to 0.025 mA with ZnONFs, further 0.067 mA for rGO and 0.07 mA for rGO and ZnONFs nanocomposite. Higher surface area to volume ratio of the rGO contributes significantly in improving the sensitivity and linear range of the OP sensor. Additionally, ZnONFs act as a catalyst and increase the surface to volume ratio and conductivity of the working electrode is enhanced due to fast electron transfer properties. The synergistic effect of both ZnONFs and rGO nanocomposite contributes to the enhancement in the peak value during electrode modification. After AChE enzyme immobilization, the oxidation peak was observed at 0.049 mA. A decrease in the current value after immobilization of the enzyme on the nanomaterial modified electrode might have occurred due to the non-insulating properties of the biomolecules.

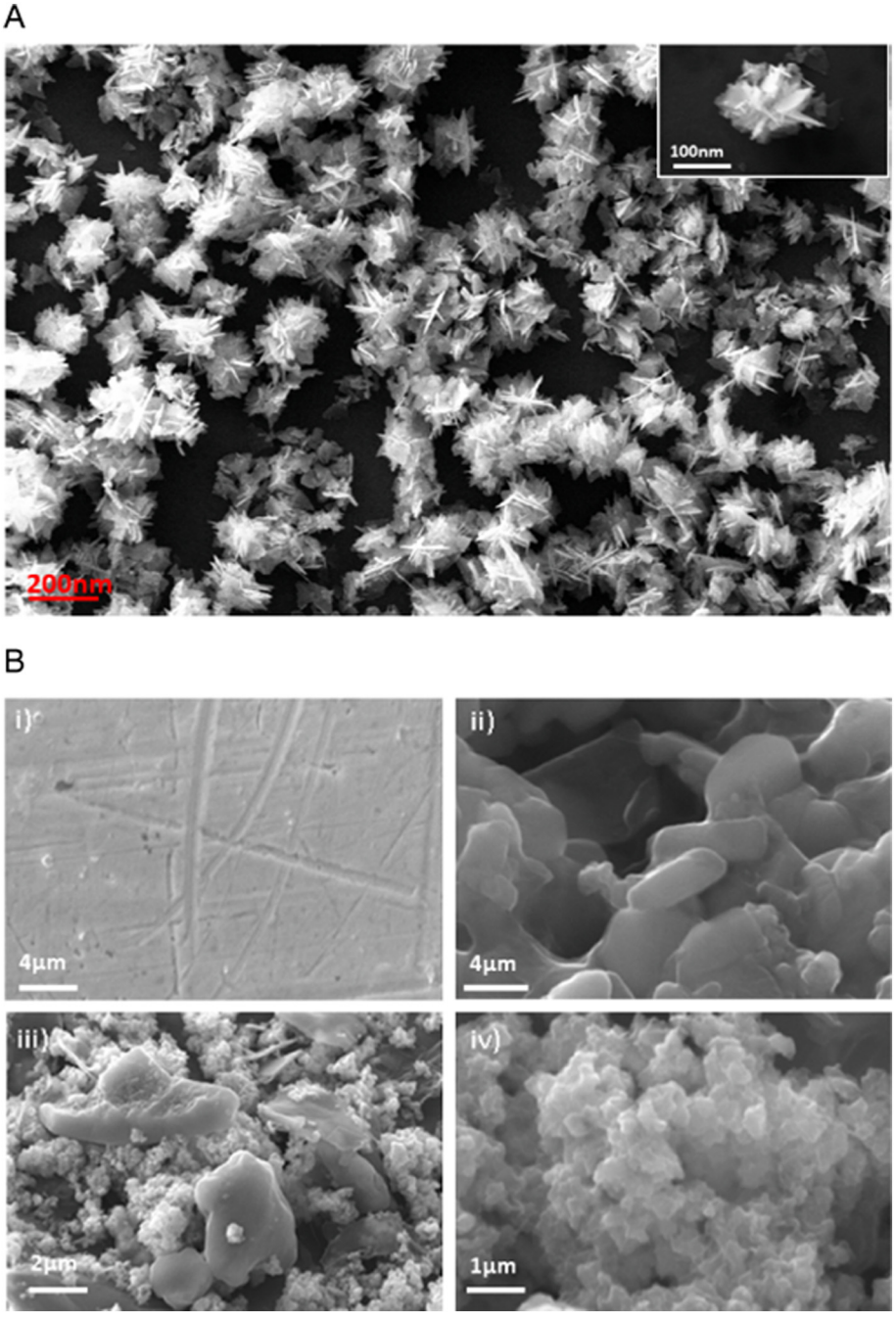

Fig. 1. A. Scanning Electron Microscopy of ZnONFs and inset shows the zoom image. B. Scanning Electron Microscopy of (i) bare Au electrode, (ii) rGO/Au electrode, (iii) ZnONFs/rGO/Au electrode, (iv) AChE/ZnONFs/rGO/Au electrode. C. Energy-dispersive X-ray spectroscopy (i) bare Au electrode, (ii) rGO/Au electrode and (iii) ZnONFs/rGO/Au electrode.

C(i)

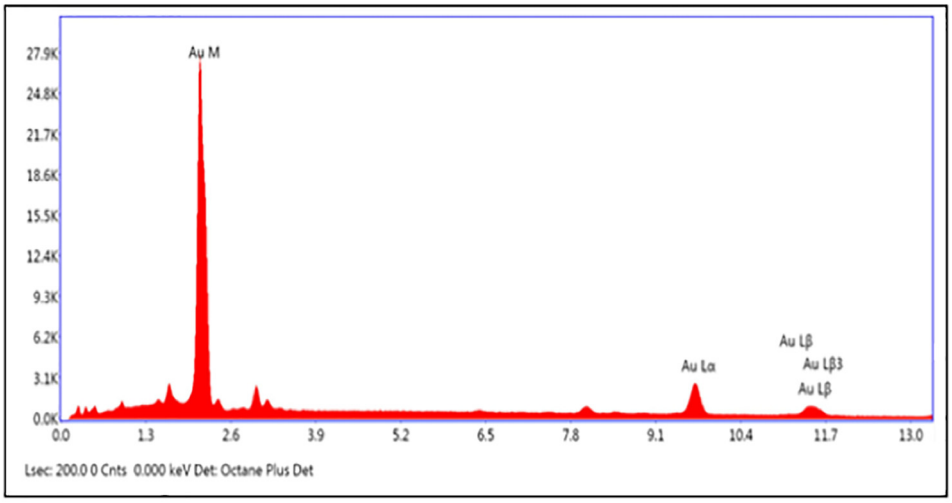

C(ii)

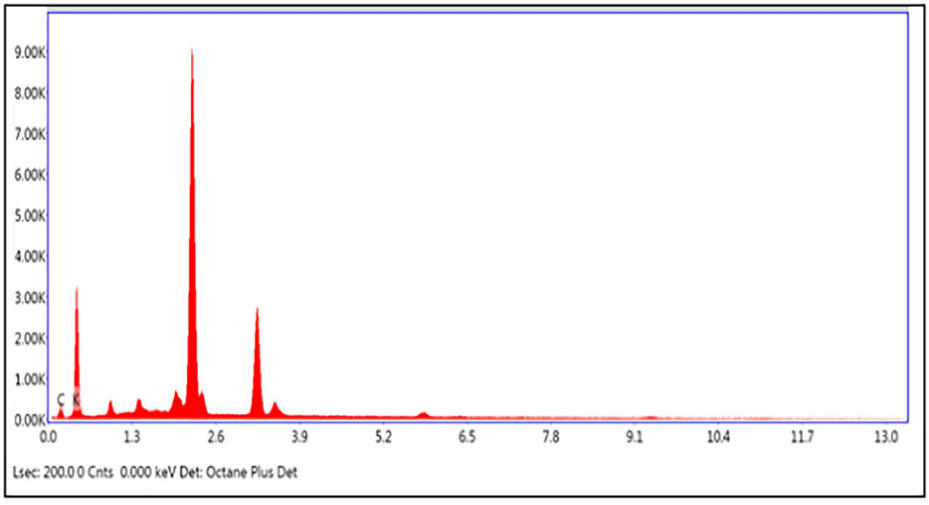

C(iii)

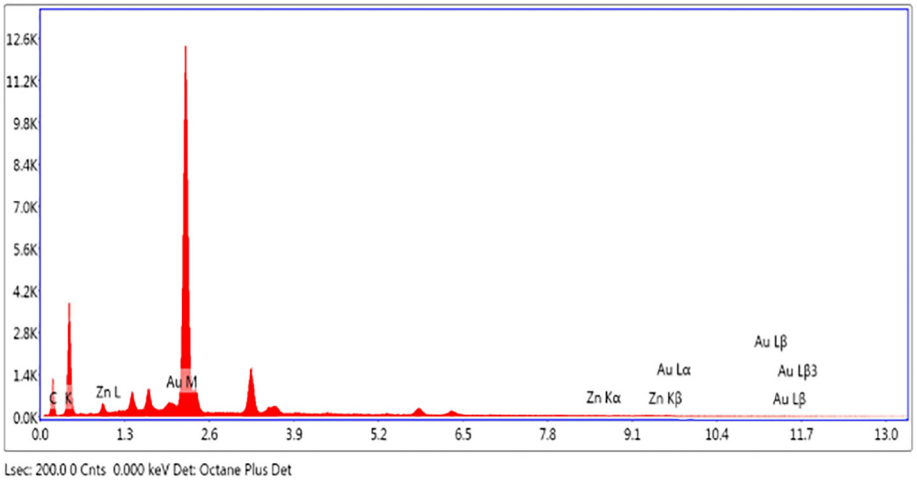

Fig. 1 (*continued*).

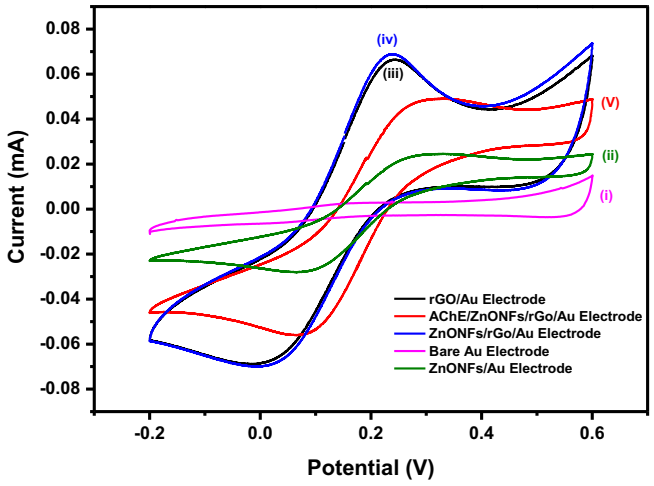

Fig. 2. Cyclic voltammetric of (i) bare Au electrode, (ii) ZnONFs/Au electrode, (iii) rGO/Au electrode, (iv) ZnONFs/rGO/Au electrode, and (v) AChE/ZnONFs/rGO/Au electrode in ferro/ferri electrolyte (5 mM) containing sodium phosphate buffer (0.5 mM) (pH 7.0) at 20 mVs^{-1}.

3.3. Electrochemical impedance spectroscopy for AChE@CHIT/ZnONFs/rGO/Au electrode

Impedance study was performed for checking the resistivity of the moderated electrode. In a Nyquist plot, the charge-transfer resistance (Rct) value is given by a semi-circle curve at a higher frequency range, whereas, the linear part represents the diffusion-limited process at a lower frequency range. Fig. 3 depicts the EIS curve for the stepwise modification of the Au electrode: Au electrode (bare) (i), rGO deposited on Au electrode (ii), decoration of ZnONFs on rGO coated Au electrode (ZnONFs/rGO/Au electrode) (iii), and immobilization of enzyme on the electrode (AChE@CHIT/ZnONFs/rGO/Au electrode) (iv). For performing the reaction Na_3PO_4 buffer solution (0.5 mM, pH 7.0) was mixed with ferro/ferri mediator (5 mM). It was observed that the Rct value obtained for the modified electrode (rGO and ZnONFs) was less than the value obtained for the bare Au electrode suggesting the higher conductivity of the developed system.

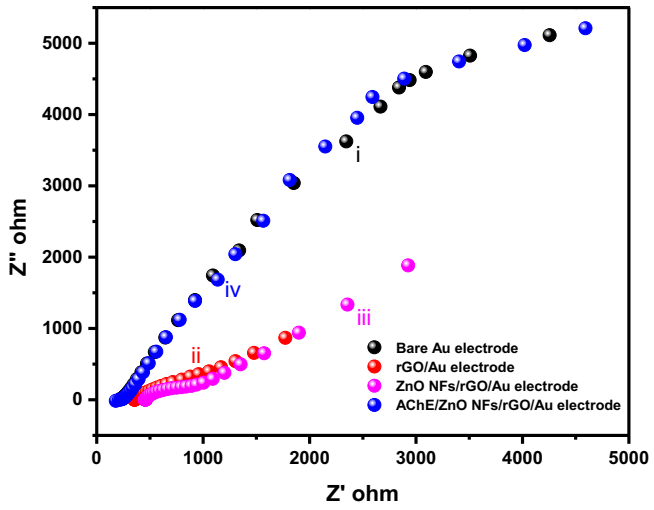

Fig. 3. Electrochemical impedance spectroscopy of (i) bare Au electrode, (ii) rGO/Au electrode, (iii) ZnONFs/rGO/Au electrode and (iv) AChE/ZnONFs/rGO/Au electrode in ferro/ferri electrolyte (5 mM) containing sodium phosphate buffer (0.5 mM; pH 7.0).

3.4. Electro-catalytic properties of the sensor for different substrate concentrations

The Square Wave Voltammetry technique was used for studying the effect of varying ATCl concentrations (1.0 nM, 10 nM, 50 nM, 100 nM, 500 nM, 750 nM, 1000 nM) on the modified AChE@CHIT/ZnONFs/rGO/Au electrode. The ATCl solution was prepared in Na_3PO_4 buffer (0.5 mM; pH 7.0) containing 5 mM ferro/ferri mediator. A potential range from −0.2 to 0.6 V was used for performing the square wave voltammetry measurements. In Fig. 4A the current value for 1 nM concentration was 40 μA and for 1000 nM the current value was about 75 μA, demonstrating a difference of 35 μA. This shows the increase in analyte concentration leads to the gradual enhancement in the current value. The LOD for the developed biosensor was obtained as 1.0 nM for the ATCl substrate. Considering different analyte concentrations and their corresponding current a calibration curve was plotted (Fig. 4B) to calculate the sensitivity (0.384 μA/nM) of the biosensor.

3.5. Effect of scan rate on the modified AChE@CHIT/ZnONFs/rGO/Au electrode

To know the electrochemical reaction rates of the analyte solutions, different scan rate studies were performed on AChE@CHIT/ZnONFs/rGO/Au electrode with CV. The study was performed with scan rates from 20 to 140 m V/s^{-} in Na_3PO_4 buffer (0.5 mM; pH 7.0) with ferro/ferri mediator. Fig. 5A depicts that the oxidation and reduction peaks

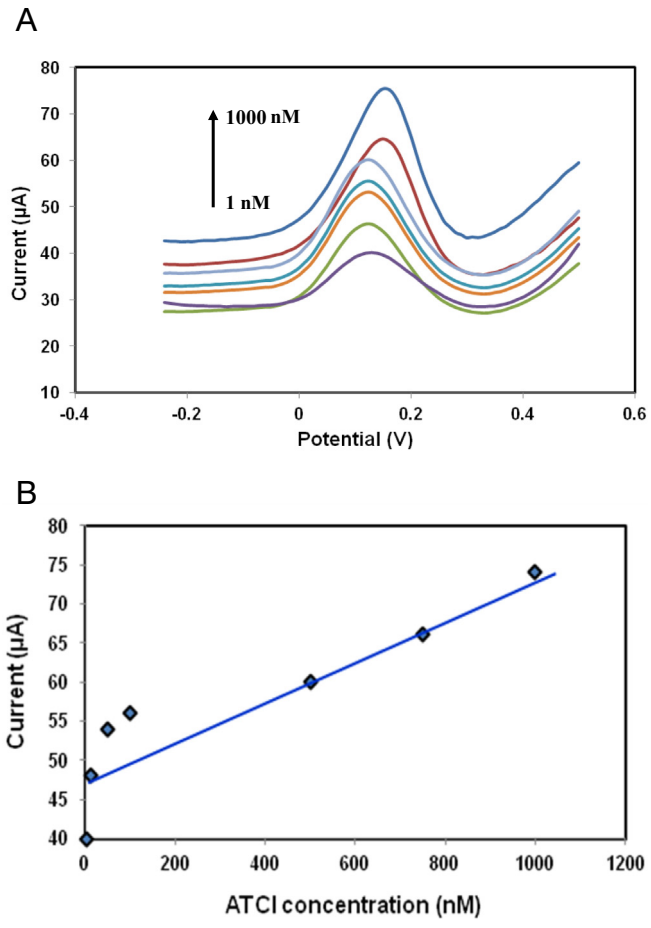

Fig. 4. A. Square Wave Voltammetry of modified AChE/ZnONFs/rGO/Au electrode with different concentration of substrate in ferro/ferri electrolyte (5 mM) containing sodium phosphate buffer (0.5 mM; pH 7.0). B. Standard curve for the different concentration of substrate vs. current response.

linearly increase with a gradual increase of scan rate at a constant potential (−0.2 to 0.6 V). It was observed that while increasing the scan rate the current value enhanced. To study the steady electron-transfer kinetics for a quasi-reversible process, a graph between oxidation current and the square root value for the scan rate was plotted (Fig. 5B). The plotted graph showed an enhancement in the oxidation current with the gradual increase in the square root function.

3.6. Optimization of the experimental parameters for AChE@CHIT/ZnONFs/rGO/Au electrode

To optimize the working conditions of the modified electrode, CV in a potential range from −0.4 to 0.6 V were generated for the AChE@CHIT/ZnONFs/rGO/Au electrode under different pH (6, 6.4, 6.8, 7.0, 7.4, and 7.8) conditions. The reactions were performed in Na_3PO_4 buffer (0.5 mM) with 5 mM ferro/ferri mediator solution. Fig. 6A represents the gradual decrease in the oxidation and reduction peaks with an increase in the pH value. The highest current was generated at pH 6.0, whereas at higher pH value the performance of the biosensor was compromised due to loss of the activity of the enzyme.

To find the optimum temperature for the working electrode, the effect of varying the temperature from 15 °C - 40 °C at an interval of 5 °C was tested on the current response of the modified AChE@CHIT/ZnONFs/rGO/Au electrode. The reaction was carried out in Na_3PO_4 buffer (0.5 mM) maintaining a pH of 6.0 with 5 mM ferro/ferri mediator. In Fig. 6B a linear change was noticed in the oxidation and reduction peaks with an increase in the temperature up to 30 °C. Raising the temperature further beyond 30 °C decreased the peaks and hence an optimum temperature of 30 °C was selected for further studies.

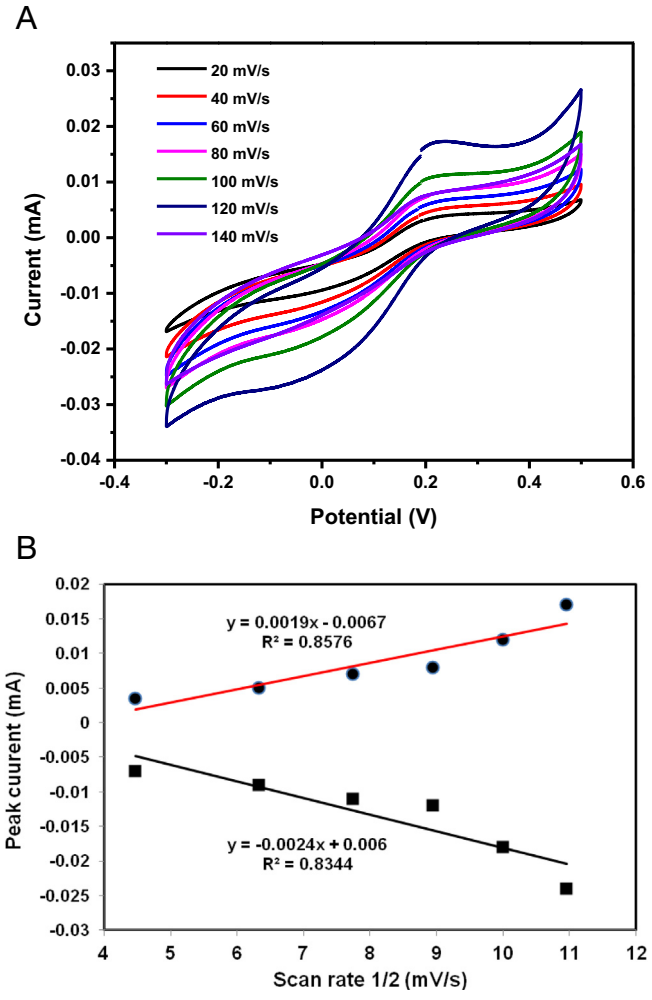

Fig. 5. A. Cyclic voltammogram recorded of AChE/ZnONFs/rGO/Au electrode scanned in 5 mM ferro/ferri electrolyte containing 0.5 mM sodium phosphate buffer (pH 7.0) with, substrate at different scan rates from 20 to 140 m V s^{-1}. B. Square root of scan rate versus the peak current plot of AChE/ZnONFs/rGO/Au electrode.

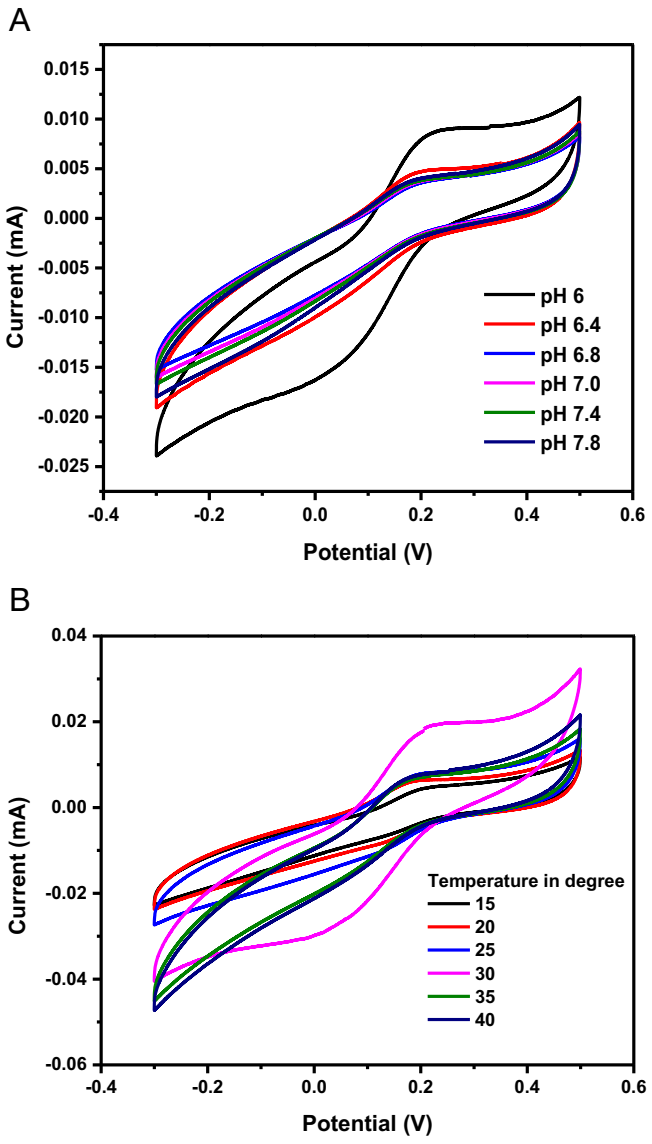

Fig. 6. A. Cyclic voltammetry study for modified AChE/ZnONFs/rGO/Au electrode with different pH values (6 to 7.8 pH). B. Cyclic voltammogram of modified AChE/ZnONFs/rGO/Au electrode with different temperature (from 15 °C to 45 °C) values in ferro/ferri electrolyte (5 mM) containing sodium phosphate buffer (0.5 mM; pH 6.0).

3.7. The electrocatalytic ability of electrode towards pesticide detection

The modified AChE/ZnONFs/rGO/Au electrode was immersed in different concentrations of standard monocrotophos solution for 10 min. Thereafter, the electrode was transferred into an electrochemical cell containing 10 mL of ferro/ferri solution (each 5.0 mL) and 1 mL of ATCl (1.0 nM) solution to perform the electrochemical studies.

The presence of ZnONFs/rGO increased the surface to volume ratio hence leading to enhancement in the enzyme loading and enhancing the catalytic property of the electrode responsible for the improved sensitivity and linearity of the OP sensor. The linear range and LOD of the biosensor were analyzed for monocrotophos with the SWV, a linear

relationship was obtained for current vs. concentrations in the concentration range of 0.01 nM to 100 nM (0.01 nM, 0.1 nM, 10 nM, 50 nM, 75 nM, and 100 nM) with the coefficient of 0.978. It was observed that increment in the pesticide concentration led to a decline in the current value because of the inhibition of enzyme activity. The obtained LOD of the biosensor for pesticide was 0.01 nM (Fig. 7A).

3.8. Selectivity testing for pesticides

The selectivity of the biosensor was examined with the detection of various types of pesticides (1) organophosphorus compounds such as monocrotophos, malathion, chlorpyrifos, parathion methyl; (2) carbamates like sevin; (3) herbicides atrazine and simazine, and

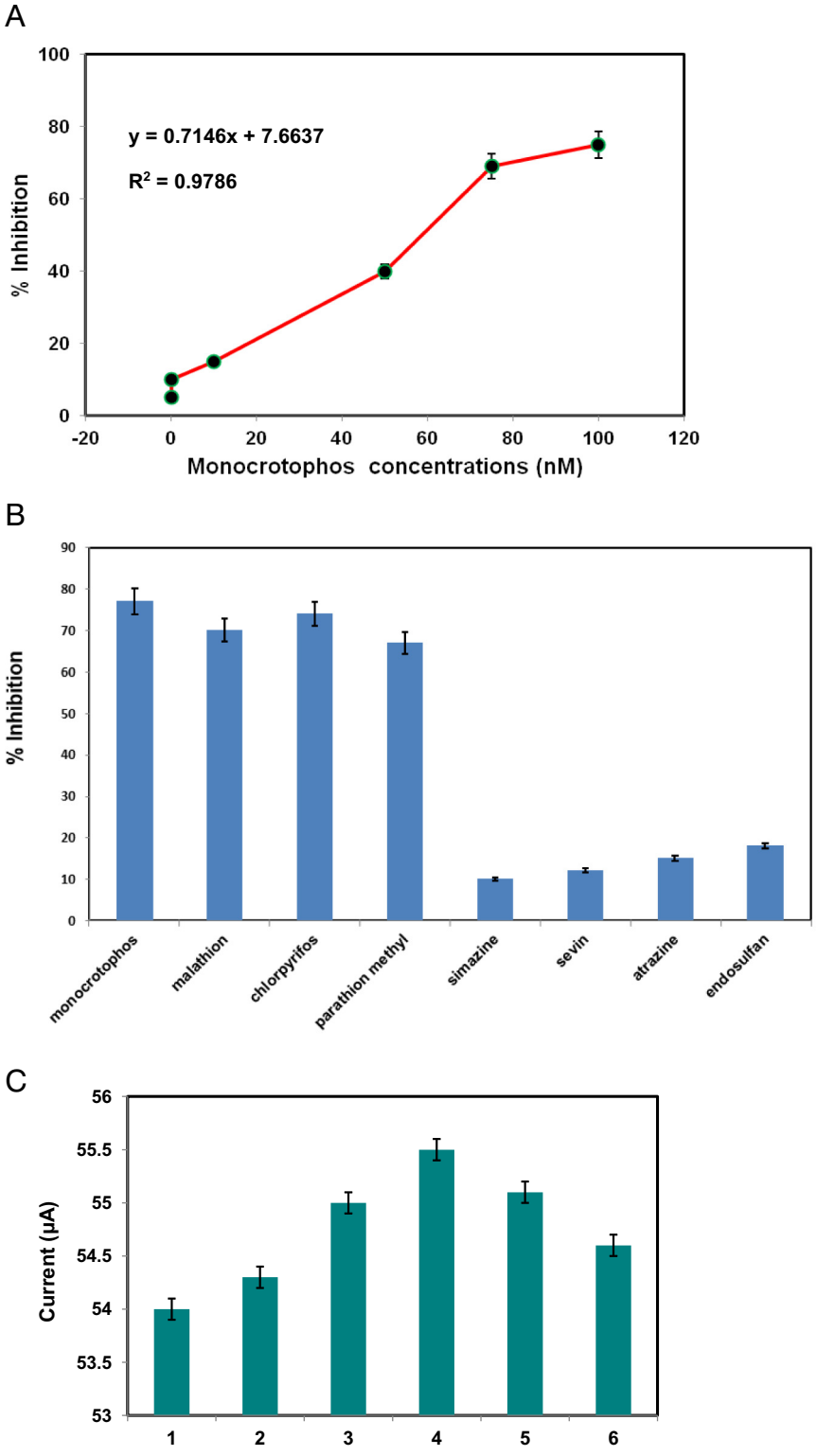

Fig. 7. A. Calibration curves for monocrotophos in 0.5 mM sodium phosphate buffer (pH 7.0) + 1.0 nM ATCl (10 min incubation time). B. Selectivity testing for various pesticides using AChE/ZnONFs/rGO/Au electrode. C. Study and evaluation of reproducibility of present electrochemical sensing platform.

Table 1
Detection of pesticide in spiked visceral samples using AChE@CHIT/ZnONFs/rGO/Au electrode.

Pesticide	Added concentration (nM/g)	Concentration found (nM/g)	Recovery (%)	SD ($n = 3$)
Monocrotophos	0.2	0.199	99.5	1.8
	0.5	0.48	98.0	2.3

(4) organochlorine e.g. endosulfan on the developed biosensor at the concentration of 100 nm. Fig. 7B clearly states that the present biosensor is not specific to a particular pesticide but is comprises a class of OP pesticides.

3.9. Regeneration of AChE after pesticide detection

Reactivation of the immobilized enzyme (AChE) is feasible with 2-PAM. In previous work, it has been reported that oximes can be used for the reactivation of the AChE [36,37].

It was observed that the modified AChE electrode inhibited by monocrotophos (0.1 nM) was able to achieve 88.95% of its original activity after washing it with cholinesterase reactivator solution (2-PAM, 4.0 mM/L) for 2 h. The reactivation procedure followed was simple and made the reuse of the enzyme electrode possible.

3.10. Measurement of OP pesticides in visceral samples

The supernatant obtained from the visceral samples was spiked with OP pesticides (0.2 nM/g and 0.5 nM/g) and their presence was detected by the developed biosensor. The developed sensor offered a high recovery from 99.5% to 98.0% (Table 1).

3.11. Stability and reproducibility of the biosensor

The storage stability of the modified electrode was evaluated for 3 months and its activity was checked once in a week. The modified AChE@CHIT/ZnONFs/rGO/Au electrode was stored dry at 4 °C, when not in use. For 2 months, there was no loss of catalytic activity, whereas, about 45% average decline in current response was observed after 2 months. Overall, the results indicated the high stability of the developed biosensor. Fig. 7C illustrates the results of the reproducibility studies assessed as the electrochemical current response for the six identical electrodes. The graph displays the current values measured with six bioelectrodes repeatedly (5 times) with an interval of 5 min between two corresponding measurements.

4. Conclusion

A biosensing platform for pesticide (Monocrotophos) detection was fabricated with a nanocomposite modified Au electrode with high sensitivity and low detection limit. A nanocomposite of ZnONFs and rGO was prepared to improve the catalytic performance of the sensor and electrodeposited onto the Au electrode. The developed biosensor demonstrated a wide linear working range from 0.01 nM to 100 nM. The sensor showed a low limit of detection (0.01 nM) and high sensitivity (0.384 μA/nM) with good reproducibility. The moderated electrode yielded reliable and reproducible results when applied for the determination of OP pesticide residues in the visceral samples. The fabricated biosensor can be used for selective detection of pesticides for forensic interest.

Supplementary data to this article can be found online at https://doi.org/10.1016/j.ijbiomac.2020.08.215.

CRediT authorship contribution statement

Mr. Amar Pal Singh performed the experiments and wrote this paper. Dr Nidhi Chauhan guided the work and contributed reagents/materials/analytical tools required for conducting experimental work. Further the paper was corrected by Ms Sapna Balayan, Dr Vinita Hooda, Dr R.K. Sarin and Dr Nidhi Chauhan.

Acknowledgements

The authors are grateful to the Department of Biotechnology (DBT), Department of Science and Technology (DST File. No. TDP/BDTD/33/2019), and Science and Engineering Research Board (SERB File No. EMR/2016/007564), India for providing their financial support in order to carry out this research work. The authors are also grateful to Forensic Science Laboratory, Delhi for encouragement and providing technical supports.

Declaration of competing interest

The author here declares that there are no competing financial interests or personal relationships that could affect the presented work.

References

[1] N. Chauhan, C.S. Pundir, An amperometric acetylcholinesterase sensor based on Fe3O4 nanoparticle/multi-walled carbon nanotube-modified ITO-coated glass plate for the detection of pesticides, Electrochim. Acta 67 (2012) 79–86, https://doi.org/10.1016/j.electacta.2012.02.012.
[2] N. Chauhan, C.S. Pundir, An amperometric biosensor based on acetylcholinesterase immobilized onto iron oxide nanoparticles/multi-walled carbon nanotubes modified gold electrode for measurement of organophosphorus insecticides, Anal. Chim. Acta 701 (2011) 66–74, https://doi.org/10.1016/j.aca.2011.06.014.
[3] R.K. Kori, K. Mandrah, W. Hasan, D.K. Patel, S.K. Roy, R.S. Yadav, Identification of markers of depression and neurotoxicity in pesticide exposed agriculture workers, J. Biochem. Mol. Toxicol. 34 (2020), e22477https://doi.org/10.1002/jbt.22477.
[4] R.M. Lane, M. Kivipelto, N.H. Greig, Acetylcholinesterase and its inhibition in Alzheimer disease, Clin. Neuropharmacol. 27 (2004) 141–149, https://doi.org/10.1097/00002826-200405000-00011.
[5] K.A. Joshi, J. Tang, R. Haddon, J. Wang, W. Chen, A. Mulchandani, A disposable biosensor for organophosphorus nerve agents based on carbon nanotubes modified thick film strip electrode, Electroanalysis 17 (2005) 54–58, https://doi.org/10.1002/elan.200403118.
[6] H. Wang, J. Wang, C. Timchalk, Y. Lin, Magnetic electrochemical immunoassays with quantum dot labels for detection of phosphorylated acetylcholinesterase in plasma, Anal. Chem. 80 (2008) 8477–8484, https://doi.org/10.1021/ac801211s.
[7] J. Bajgar, Organophosphates/nerve agent poisoning: mechanism of action, diagnosis, prophylaxis, and treatment, Adv. Clin. Chem. 38 (2004) 151–216.
[8] C.H. Srinivas Rao, V. Venkateswarlu, T. Surender, M. Eddleston, N.A. Buckley, Pesticide poisoning in south India: opportunities for prevention and improved medical management, Tropical Med. Int. Health 10 (2005) 581–588, https://doi.org/10.1111/j.1365-3156.2005.01412.x.
[9] R. García-Repetto, Sample preparation for pesticide analysis in a forensic toxicology laboratory: a review, J. Forsenic. Sci. Dig. Invest. 1 (2018) 27–45, https://doi.org/10.29199/fsdi.101016.
[10] M. Eddleston, Poisoning by pesticides, Medicine 48 (2020) 214–217, https://doi.org/10.1016/j.mpmed.2019.12.019.
[11] F. Hernandez, J. Sancho, O. Pozo, Critical review of the application of liquid chromatography/mass spectrometry to the determination of pesticide residues in biological samples, Anal. Bioanal. Chem. 382 (2005) 934–946.
[12] S. Yao, A. Meyer, G. Henze, Comparison of amperometric and UV-spectrophotometric monitoring in the HPLC analysis of pesticides, Fresenius J. Anal. Chem. 339 (1991) 207–211, https://doi.org/10.1007/BF00325738.
[13] Q. Wang, Y. Xiong, L. Lou, Biosensor for detection of pesticide residue, Am. J. Nano Res. Appl 3 (2015) 18–22.
[14] V. Dhull, A. Gahlaut, N. Dilbaghi, V. Hooda, Acetylcholinesterase biosensors for electrochemical detection of organophosphorus compounds: a review, Biochem. Res. Int. (2013)https://doi.org/10.1155/2013/73150.
[15] S. Andreescu, J.L. Marty, Twenty years research in cholinesterase biosensors: from basic research to practical applications, Biomol. Eng. 23 (2006) 1–5, https://doi.org/10.1016/j.bioeng.2006.01.001.

[16] Y. Li, Y. Bai, G. Han, M. Li, Porous-reduced graphene oxide for fabricating an amperometric acetylcholinesterase biosensor, Sensors Actuators B Chem. 185 (2013) 706–712, https://doi.org/10.1016/j.snb.2013.05.061.
[17] R. Buiculescu, N.A. Chaniotakis, The stabilization of Au NP–AChE nanocomposites by biosilica encapsulation for the development of a thiocholine biosensor, Bioelectrochemistry 86 (2012) 72–77, https://doi.org/10.1016/j.bioelechem.2012.02.005.
[18] N. Chauhan, J. Narang, C.S. Pundir, Immobilization of rat brain acetylcholinesterase on porous gold-nanoparticle–CaCO3 hybrid material modified Au electrode for detection of organophosphorous insecticides, Int. J. Biol. Macromol. 49 (2011) 923–929, https://doi.org/10.1016/j.ijbiomac.2011.08.006.
[19] N. Chauhan, J. Narang, C.S. Pundir, Immobilization of rat brain acetylcholinesterase on ZnS and poly (indole-5-carboxylic acid) modified Au electrode for detection of organophosphorus insecticides, Biosens. Bioelectron. 29 (2011) 82–88, https://doi.org/10.1016/j.bios.2011.07.070.
[20] C.S. Pundir, N. Chauhan, Acetylcholinesterase inhibition-based biosensors for pesticide determination: a review, Anal. Biochem. 429 (2012) 19–31, https://doi.org/10.1016/j.ab.2012.06.025.
[21] C. Zhu, G. Yang, H. Li, D. Du, Y. Lin, Electrochemical sensors and biosensors based on nanomaterials and nanostructures, Anal. Chem. 87 (2015) 230–249, https://doi.org/10.1021/ac5039863.
[22] S. Chawla, R. Rawal, S. Sharma, C.S. Pundir, An amperometric biosensor based on laccase immobilized onto nickel nanoparticles/carboxylated multiwalled carbon nanotubes/polyaniline modified gold electrode for determination of phenolic content in fruit juices, Biochem. Eng. J. 68 (2012) 76–84, https://doi.org/10.1016/j.bej.2012.07.008.
[23] Q. Xia, Y. Huang, X. Lin, S. Zhu, Y. Fu, Highly sensitive d-alanine electrochemical biosensor based on functionalized multi-walled carbon nanotubes and d-amino acid oxidase, Biochem. Eng. J. 113 (2016) 1–6, https://doi.org/10.1016/j.bej.2016.05.003.
[24] A.Y. Khan, S.B. Noronha, R. Bandyopadhyaya, Glucose oxidase enzyme immobilized porous silica for improved performance of a glucose biosensor, Biochem. Eng. J. 91 (2014) 78–85, https://doi.org/10.1016/j.bej.2014.07.011.
[25] M. Chen, C. Hou, D. Huo, H. Fa, Y. Zhao, C. Shen, A sensitive electrochemical DNA biosensor based on three-dimensional nitrogen-doped graphene and Fe3O4 nanoparticles, Sensors Actuators B Chem. 239 (2017) 421–429, https://doi.org/10.1016/j.snb.2016.08.036.
[26] A.P. Periasamy, Y. Umasankar, S.M. Chen, Nanomaterials-acetylcholinesterase enzyme matrices for organophosphorus pesticides electrochemical sensors: a review, Sensors 9 (2009) 4034–4055, https://doi.org/10.3390/s90604034.
[27] L. Ma, L. Zhou, Y. He, L. Wang, Z. Huang, Y. Jiang, J. Gao, Hierarchical nanocomposites with an N-doped carbon shell and bimetal core: novel enzyme nanocarriers for electrochemical pesticide detection, Biosens. Bioelectron. 121 (2018) 166–173, https://doi.org/10.1016/j.bios.2018.08.038.
[28] L. Ma, Y. He, Y. Wang, Y. Wang, R. Li, Z. Huang, Y. Jiang, J. Gao, Nanocomposites of Pt nanoparticles anchored on UiO66-NH2 as carriers to construct acetylcholinesterase biosensors for organophosphorus pesticide detection, Electrochim. Acta 318 (2019) 525–533, https://doi.org/10.1016/j.electacta.2019.06.110.
[29] F. Zhao, Y. Yao, C. Jiang, Y. Shao, D. Barceló, Y. Ying, J. Ping, Self-reduction bimetallic nanoparticles on ultrathin MXene nanosheets as functional platform for pesticide sensing, J. Hazard. Mater. 384 (2020), 121358https://doi.org/10.1016/j.jhazmat.2019.121358.
[30] W. Putzbach, N.J. Ronkainen, Immobilization techniques in the fabrication of nanomaterial-based electrochemical biosensors: a review, Sensors (Switzerland) 13 (2013) 4811–4840, https://doi.org/10.3390/s130404811.
[31] A. Kumar, S. Arora, N. Mogha, S.S. Al-Deyab, Z.A. Ansari, S.G. Ansari, Glutathione coated zinc oxide nanoparticles: a promising material for pesticide detection, Energy Environ. Focus. 2 (2013) 101–107, https://doi.org/10.1166/eef.2013.1034.
[32] E. Prokhorov, G. Luna-Bárcenas, J.B. González-Campos, Y. Kovalenko, Z.Y. García-Carvajal, J. Mota-Morales, Proton conductivity and relaxation properties of chitosan-acetate films, Electrochim. Acta 215 (2016) 600–608, https://doi.org/10.1016/j.electacta.2016.08.148.
[33] N. Cao, Y. Zhang, Study of reduced graphene oxide preparation by Hummers' method and related characterization, J. Nanomater. (2015)https://doi.org/10.1155/2015/168125.
[34] R. Wahab, Y.S. Kim, H.S. Shin, Fabrication, characterization and growth mechanism of heterostructured zinc oxide nanostructures via solution method, Curr. Appl. Phys. 11 (2011) 334–340, https://doi.org/10.1016/j.cap.2010.07.030.
[35] S. Gupta, A. Tiwari, U. Jain, N. Chauhan, Synergistic effect of 2D material coated Pt nanoparticles with PEDOT polymer on electrode surface interface for a sensitive label free Helicobacter pylori CagA (Ag-Ab) immunosensing, Mater. Sci. Eng. C 103 (2019), 109733https://doi.org/10.1016/j.msec.2019.05.018.
[36] K.C. Gulla, M.D. Gouda, M.S. Thakur, N.G. Karanth, Reactivation of immobilized acetyl cholinesterase in an amperometric biosensor for organophosphorus pesticide, Biochim. Biophys. Acta Protein Struct. Mol. Enzymol. 1597 (2002) 133–139, https://doi.org/10.1016/S0167-4838(02)00268-6.
[37] K. Anitha, S.V. Mohan, S.J. Reddy, Development of acetylcholinesterase silica sol–gel immobilized biosensor—an application towards oxydemeton methyl detection, Biosens. Bioelectron. 20 (2004) 848–856, https://doi.org/10.1016/j.bios.2004.03.024.